Middle-East Journal of Scientific Research 11 (4): 461-469, 2012
ISSN 1990-9233

Thermal and Hydraulic Behavior of Rectangular Enclosures Under the Effect of Magnetic Field

Hamed Ashoori

Department of Civil Engineering, Gonbad Kavoos Branch, Islamic Azad University, Gonbad Kavoos, Iran

Abstract: A 2-D computational analysis of steady magnetohydrodynamic free convection in a rectangular enclosure with a fixed aspect ratio (length/height=4) and filled with an electrically conducting fluid has been performed. The enclosure is differentially heated at two opposite vertical walls while the horizontal walls are at adiabatic condition. A uniform magnetic field with different magnitudes and orientations is applied. The governing equations (mass, momentum and energy) are formulated and solved by a Finite Volume Method (FVM) subjected appropriate boundary conditions. A parametric study illustrating the influence of Grashof number, Prantdl number of fluid, Hartmann number and orientation of magnetic field on the flow and heat transfer characteristic such as average Nusselt number, streamlines and isotherms is performed. It is observed that Nu rises with increasing Grashof and Prandtl numbers and decreasing Hartmann and orientation of magnetic field.

Key words: Rectangular Cavity · Magnetohydrodynamic free convection · Hartmann number

INTRODUCTION

The effect of the magnetic field has many applications in engineering problems such as plasma studies, nuclear reactors, boundary layer control in the field of aerodynamics, geothermal energy extraction and electromagnetic launch technology. Semiconducting and superconducting materials are special types of materials that they are used in electromagnetic launch technology. Some applications in launch technology include superconducting inductive pulsed power supply for electromagnetic launchers, electromagnetic launcher with a high temperature superconducting which launch a shuttle, superconducting electromagnetic projectile launchers, superconducting ceramic rails and semiconductor armature.

In plasma studies the liquid metal is used as coolant for fusion reactor blanket and due to liquid metal susceptibility to the magnetic field that is present in the blanket, its heat transfer rate and flow pattern are influenced. In manufacturing of semiconductors the special manufacturing process is used like Bridgman configuration. This configuration is one of the important methods for growth of superconductor and semiconductor single crystals. In the horizontal Bridgman technique, the molten crystal is contained in a crucible which is withdrawn horizontally from a furnace. Thus the melt is subject to a horizontal temperature gradient, which drives the end wall convection. In industry the quality of crystal is affected adversely by instabilities in the melt phase because instabilities impose temperature fluctuations at the solidification front and lead to striations in the crystalline product. It is well known that applying magnetic field to the system leads to damping unavoidable hydrodynamic movement and consequently growing high quality crystals. The external magnetic field effect on convection heat transfer by slowing or inhibiting the motion of liquid and this cause to decrease the convection heat transfer rate. In general, the quality and homogeneity of single crystals grown from dropped semiconductor melts are very important and interesting for manufactures of semi- and superconductors. Therefore, analysis of flow and heat transfer of liquid metals in cavities subjected to external magnetic field is interesting for researchers in this field.

Many investigators experimentally, numerically and analytically studied the natural convection of electrically conducted fluids in presence of magnetic field. For instance, Rudraiah *et al*. [1] numerically studied the effect of a transverse magnetic field on the natural - convection flow inside a rectangular cavity with adiabatic horizontal walls and isothermal vertical walls. They found that a

Corresponding Auhtor: Hamed Ashoori, Department of Civil Engineering, Gonbad Kavoos Branch, Islamic Azad University, Gonbad Kavoos, Iran.

circulating flow is formed with a relatively weak magnetic field that the convection is suppressed and the role of convective heat transfer is decreased when the magnetic field strength increases. Pirmohammadi *et al*. [4] have studied the effect of a magnetic field on the buoyancy driven convection in a differentially heated square cavity. The results showed that the flow characteristics inside the cavity and heat transfer mechanism depend strongly upon both the strength of the Rayleigh number and magnetic field. For a review of other numerical, experimental and analytical studies and interested reader may refer to Refs [3-13].

Most of the previous studies apply magnetic field in perpendicular or parallel direction with gravity vector, no more existing studies apply magnetic field in the direction inclined with gravity vector. When the direction of a magnetic field is perpendicular to the gravity vector, the flow induced by the buoyant force crosses it. In that case, in the momentum equation for the vertical velocity component an additional term for the electromagnetic force appears. Therefore, the boundary layer approximation is applicable, so the equation is simplified as in [3-4]. However, for the case when the direction of magnetic field is parallel to gravity vector, a term for the electromagnetic force appear in the momentum equation for horizontal velocity component and the buoyancy force appear in the momentum equation for the vertical velocity component. Therefore, the momentum equations for velocity components must be solved as in [7]. When the direction of the magnetic field is tilted in angle with the gravity vector, it interact with the velocity components that are parallel and perpendicular to the gravity vector and a term for magnetic force appears in the momentum equations for both velocity components and buoyancy force appear in the momentum equation for the vertical velocity component. Therefore, the vertical momentum equation will consist electromagnetic field and buoyancy term and horizontal momentum equation contains only electromagnetic force term.

The main scope of the present paper is to study the effect of orientation of magnetic field on thermal and hydrodynamic behavior of a rectangular cavity. Two different working fluid with Prandtl number of 0.15 and 0.015 will be compared. The fluid flow is in laminar regime and it is assumed to be Newtonian. The governing equations for heat transfer and flow will be solved using finite volume approach in a collocated grid. The current research will evaluate the effect of Hartmann and Grashof numbers as well as orientation of magnetic field, on stream function and temperature contour as well as Nusselt number of hot wall. It is shown that using working fluid with higher Prandtl numbers leads to higher Nusselt numbers. Furthermore, increasing Grashof number, decreasing orientation angle of magnetic field and decreasing Hartmann number cause the Nusselt number decreases.

Mathematical Modeling and Boundary Conditions: Figure 1 shows a schematic diagram of the system considered in the present study. The system consists of a rectangular cavity with length of L and height of $H = L/4$. A Cartesian co-ordinate system is used with origin at the lower left corner of computational domain. The left and right walls of cavity are hot and cold and they are considered at a constant temperatures of T_h and T_c respectively. The horizontal walls are kept adiabatic. The flow in the rectangular cavity is subject to a uniform magnetic field of B_0. The orientation of magnetic field forms an angle α with horizontal axis. All four walls are electrically insulated boundaries and the fluid within the cavity is assumed to have constant properties except insofar as the buoyancy is concerned, i.e. the Boussinesq approximation of linear temperature dependence of density is utilized. It is worth mentioning that the fluid in the enclosure received both the electromagnetic force resulting from convection of fluid in an uniform magnetic field and resulting from heat transfer through side walls.

By using Ohm's law without Hall effect and electrically insulated boundaries, the magnetic current density is

$$J = \sigma (V \times B) \tag{1}$$

The electromagnetic force is:

$$F_{EM} = J \times B \tag{2}$$

The ensemble average of the fluctuation electromagnetic force in the momentum equation was neglected. The induced magnetic field is small compared to the applied magnetic field, so $B = B_0$ and $B = B_x i + B_y j$ Where the magnitude and orientation angle of magnetic field with horizontal axis are

$$\alpha = \arctan\left(\frac{B_y}{B_x}\right), \qquad B_0 = \sqrt{{B_x}^2 + {B_y}^2} \tag{3}$$

The two-dimensional governing equation for an incompressible, Newtonian liquid in laminar regime and in steady state conditions is given by:

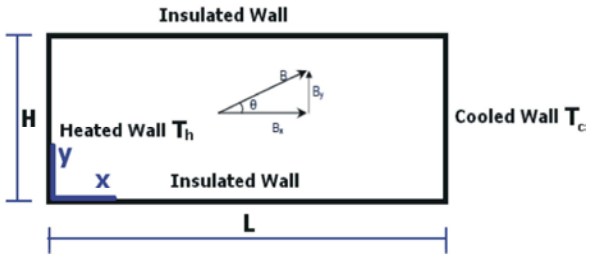

Fig. 1: Schematic of computational domain and coordinate system

Continuity equation:

$$\frac{\partial u}{\partial x}+\frac{\partial v}{\partial y}=0 \tag{4}$$

X-Momentum equation:

$$\rho\left(u\frac{\partial u}{\partial x}+v\frac{\partial u}{\partial y}\right)=-\frac{\partial p}{\partial x}+\frac{\partial}{\partial x}\left(\mu\frac{\partial u}{\partial x}\right)+\frac{\partial}{\partial y}\left(\mu\frac{\partial u}{\partial y}\right)+\sigma B^2\left(v\cos(\alpha)\sin(\alpha)-u\sin^2(\alpha)\right) \tag{5}$$

Y-Momentum equation:

$$\rho\left(u\frac{\partial v}{\partial x}+v\frac{\partial v}{\partial y}\right)=-\frac{\partial p}{\partial y}+\frac{\partial}{\partial x}\left(\mu\frac{\partial v}{\partial x}\right)+\frac{\partial}{\partial y}\left(\mu\frac{\partial v}{\partial y}\right)+\rho g\beta\left(T-T_c\right)+\sigma B^2\left(u\cos(\alpha)\sin(\alpha)-v\cos^2(\alpha)\right) \tag{6}$$

Energy:

$$\left(\rho C_p\right)\left(u\frac{\partial T}{\partial x}+v\frac{\partial T}{\partial y}\right)=\frac{\partial}{\partial x}\left(k\frac{\partial T}{\partial x}\right)+\frac{\partial}{\partial y}\left(k\frac{\partial T}{\partial y}\right) \tag{7}$$

Where u,v are velocity components in x, y directions, respectively. p and T are pressure and temperature, respectively. ρ, g, k, C_p, β and σ re the density, acceleration due to gravity, thermal conductivity of liquid, heat capacitance of the liquid in the cavity, thermal expansion coefficient and electrical conductivity of fluid, respectively. It is important to note that in thermal energy equation the radiation heat transfer, joule heating, pressure work and viscous dissipation are ignored. The boundary conditions are:

$$\begin{aligned}
&@\ x=0 \quad u=v=0\ and \quad T=T_h\\
&@\ x=L \quad u=v=0\ and \quad T=T_c\\
&@\ y=0 \quad u=v=0\ and \quad \frac{\partial T}{\partial y}=0\\
&@\ y=H \quad u=v=0\ and \quad \frac{\partial T}{\partial y}=0
\end{aligned} \tag{8a-d}$$

The local Nusselt number at the heated wall is evaluated by the following expression in dimensional form as:

$$Nu_{local}=\frac{hH}{k} \tag{9}$$

By using the following dimensionless variables the above equations and boundary conditions take the following form:

$$\bar{x}=\frac{x}{L},\ \bar{y}=\frac{y}{H},\ \bar{u}=\frac{u}{\mu/\rho H},\ \bar{v}=\frac{v}{\mu/\rho H},\ \bar{p}=\frac{p}{\rho\left(\mu/\rho H\right)^2},\ \theta=\frac{T-T_c}{T_h-T_c} \tag{10}$$

Continuity equation:

$$\frac{\partial \bar{u}}{\partial \bar{x}}+\frac{\partial \bar{v}}{\partial \bar{y}}=0 \tag{11}$$

X-Momentum equation:

$$\bar{u}\frac{\partial \bar{u}}{\partial \bar{x}}+\bar{v}\frac{\partial \bar{u}}{\partial \bar{y}}=-\frac{\partial \bar{p}}{\partial \bar{x}}+\frac{\partial^2 \bar{u}}{\partial \bar{x}^2}+\frac{\partial^2 \bar{v}}{\partial \bar{y}^2}+Ha^2\left(\bar{v}\cos(\alpha)\sin(\alpha)-\bar{u}\sin^2(\alpha)\right) \tag{12}$$

Y-Momentum equation:

$$\bar{u}\frac{\partial \bar{v}}{\partial \bar{x}}+\bar{v}\frac{\partial \bar{v}}{\partial \bar{y}}=-\frac{\partial \bar{p}}{\partial \bar{y}}+\frac{\partial^2 \bar{v}}{\partial \bar{x}^2}+\frac{\partial^2 \bar{u}}{\partial \bar{y}^2}+Gr\theta+Ha^2\left(\bar{u}\cos(\alpha)\sin(\alpha)-\bar{v}\cos^2(\alpha)\right) \tag{13}$$

Energy:

$$\bar{u}\frac{\partial \theta}{\partial \bar{x}}+\bar{v}\frac{\partial \theta}{\partial \bar{y}}=\frac{1}{\mathrm{Pr}}\left(\frac{\partial^2 \theta}{\partial \bar{x}^2}+\frac{\partial^2 \theta}{\partial \bar{y}^2}\right) \tag{14}$$

With following boundary conditions

$$\begin{aligned}
&@\ \bar{x}=0 \quad \bar{u}=\bar{v}=0\ and \quad \theta=1\\
&@\ \bar{x}=4 \quad \bar{u}=\bar{v}=0\ and \quad \theta=0\\
&@\ \bar{y}=0 \quad \bar{u}=\bar{v}=0\ and \quad \frac{\partial \theta}{\partial \bar{y}}=0\\
&@\ \bar{y}=1 \quad \bar{u}=\bar{v}=0\ and \quad \frac{\partial \theta}{\partial \bar{y}}=0
\end{aligned} \tag{15a-d}$$

Where

$$Gr=\frac{g\beta\left(T_h-T_c\right)H^3\rho^2}{\mu^2},\ \mathrm{Pr}=\frac{\rho c_p}{k},\ Ha=B_0H\sqrt{\sigma/\mu} \tag{16}$$

Finally the average Nusselt number on the hot wall can be calculated using:

$$Nu=\int_0^1\left.\frac{\partial \theta}{\partial \bar{x}}\right|_{x=0}d\bar{y} \tag{17}$$

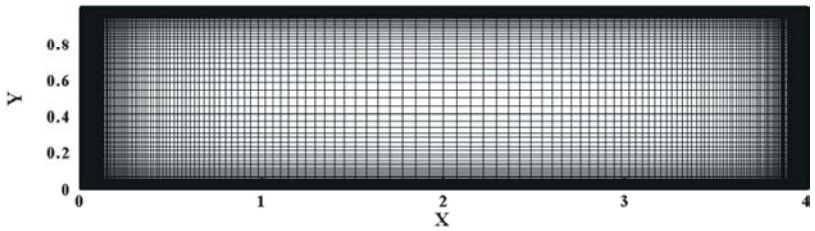

Fig. 2: Computational grid

Numerical Solution and Validation: Equations (11)-(14) with their associated boundary conditions were solved numerically using a finite volume code based on collocated grid on a structured grid. In order to correctly capture the viscous layer, the grids near the solid walls were refined. Figure 2 shows the grid configuration used in the present simulation. Discretized equations were derived by integrating the governing equations over each control volume and then approximating the resulting integrals using multidimensional linear reconstruction approach [14]. The convective terms are calculated from face values by means of QUICK [15] scheme and a second-order centered scheme was used to calculated diffusive terms in the governing equations. The resulting scalar system of equations for dependent variable in each cell was solved using a point implicit (Gauss-Seidel) linear equation in conjunction with an algebraic multigrid (AMG) method. The SIMPLE [16] (Semi-implicit method for pressure-linked equations) algorithm was used to accomplish the pressure- velocity coupling. The convergence of code was declared when the residual of each component of velocity vector, pressure and temperature become 10^{-7}, 10^{-5} and 10^{-11}, respectively.

$$\sum_{i=0}^{N_x}\sum_{j=0}^{N_y}\left|V(i,j)-V_0(i,j)\right|\le 10^{-7}$$
$$\sum_{i=0}^{N_x}\sum_{j=0}^{N_y}\left|p(i,j)-p_0(i,j)\right|\le 10^{-5}$$
$$\sum_{i=0}^{N_x}\sum_{j=0}^{N_y}\left|T(i,j)-T_0(i,j)\right|\le 10^{-11} \qquad \text{(26 a-c)}$$

Where N_x and N_y are number of grid in x and y directions, respectively. The subscripts i, j refer to ith and jth grid-cells in the x and y directions, respectively. Index° refers to the previous iteration. As second criterion for convergence and to further ensure the accuracy of the computation, the total heat transfer rate was examined through comparing the total input and output heats from the hot and cold walls.

Table 1: Girds independency study

	Number of grids	Nu	ψ_{max}
$Gr = 10^5$	30×20	0.19.26	5.69
$\alpha = 0$	40×30	0.21560	7.56
$Ha = 80$	50×40	0.24990	8.19
	60×50	0.25150	8.30
$Gr = 10^7$	30×20	0.46980	121.36
$\alpha = 90$	40×30	0.59870	155.36
$Ha = 40$	50×40	0.68490	162.94
	60×50	0.69130	163.78

To obtain better accuracy in the simulations, four quadrilateral grids with total sizes of 30×20 (coarse), 40×30 (medium), 50×40 (fine), 60×50 (very fine) were generated by discretizing the computational domain, for the grid sensitivity study. Table 1 shows the comparison between the calculated Nusselt number of the hot wall and maximum value of stream function in the computational domain in each grid.

As seen the maximum deviations among third and fourth grid were very small, hence the solution becomes independent of grid size in third grid. Therefore, based on aforementioned parameters for grid independency test, the third configuration with total number of 50×40 cells seemed to be adequate to accurately capture fluid flow and heat transfer behaviors in the cavity and further increasing the grids will have negligible effect on the solution and results.

In order to check the accuracy and reliability of numerical procedure, the results should validate with previous data from literature. Therefore, we analyzed a system composed of fluid in an enclosure with different Ra numbers and Pr= 0.7. this system has been studied by other research groups, including Davis [17], Markatos and Pericleous [18] and Hadjisophocleous *et al*. [19]. Table 2 shows a comparison of calculated maximum velocity components and average Nusselt number with the data in the literature base of same dimensions and boundary conditions. Comparison of the previous data and present numerical results indicate that the results of our numerical

Table 2: Comparison of present numerical results with previous works in an enclosure for Pr=0.7 with different Rayleigh numbers

	Present	Davis [17]	Hadjisophocleous *et al.* [19]	Markatos and Pericleous [18]
	$Ra = 10^4$			
u_{max}	16.15	16.178	15.955	16.18
y	0.819	0.823	0.814	0.832
v_{max}	19.64	19.617	18.894	19.44
x	0.112	0.119	0.103	0.113
$N\overline{u}$	2.241	2.243	2.29	2.201
	$Ra = 10^5$			
u_{max}	36.729	34.73	37.144	35.73
y	0.858	0.855	0.855	0.857
v_{max}	68.269	68.59	68.91	69.08
x	0.063	0.066	0.061	0.067
$N\overline{u}$	4.513	4.519	4.964	4.430
	$Ra = 10^6$			
u_{max}	66.462	64.63	66.42	68.81
y	0.86851	0.85	0.897	0.872
v_{max}	222.341	217.36	226.4	221.8
x	0.03804	0.0379	0.0206	0.0375
$N\overline{u}$	8.756	8.799	10.39	8.754

code are in good agreement with available results in the literature. The above code verification tests indicate that the present numerical simulations are sufficiently valid for this study.

RESULTS AND DISCUSSIONS

Finite Volume simulation is applied to perform the analysis of laminar free convection heat transfer and fluid flow in a rectangular cavity under the effect of magnetic field. Effects of the parameters such as Grashof number (Gr), Hartmann number (Ha), orientation of magnetic field and Prandtl number of fluid (Pr) on heat transfer and fluid flow inside the cavity have been studied. We have presented the results in two sections. The first section has focused on flow and temperature fields, which contains streamlines and isotherms for the different cases. Heat transfer including average Nusselt number at the heated wall has been discussed in the following section. The ranges of Gr, Ha and α for this investigation vary from 10^5 to 10^7, 0 to 80 and 0 to 90, respectively while the prandtl number is kept fixed at 0.015 and 0.15.

A distinct advantage of numerical simulations is that they can be used to provide a full and detailed picture of the model flow. The influence of Grashof number Gr (from $Gr = 10^5$ to $Gr = 10^7$) on streamlines as well as isotherms for the present configuration at Ha = 0, Pr = 0.015, $\alpha = 0$ has been demonstrated in Fig. 3(a,b). The flow with $Gr = 10^5$ has been affected by the buoyancy force, thus creating a vortex at the center of cavity. This region decreases with increasing Grashof number as shown in Fig. 3(a). For $Gr = 1.4\times10^6$, the size of the existing

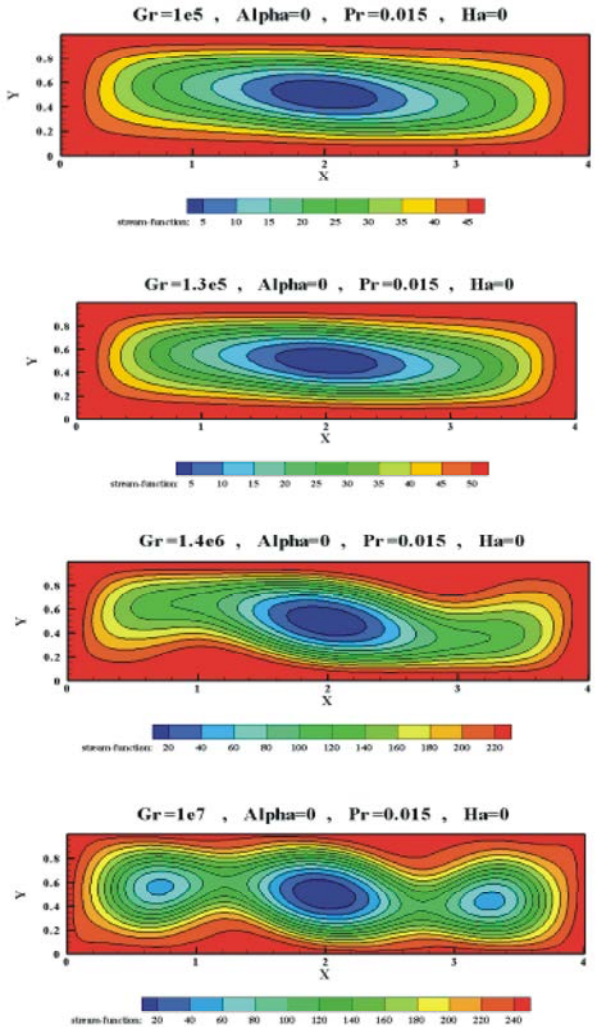

Fig. 3a: Effect of Grashof number on streamlines inside the cavity

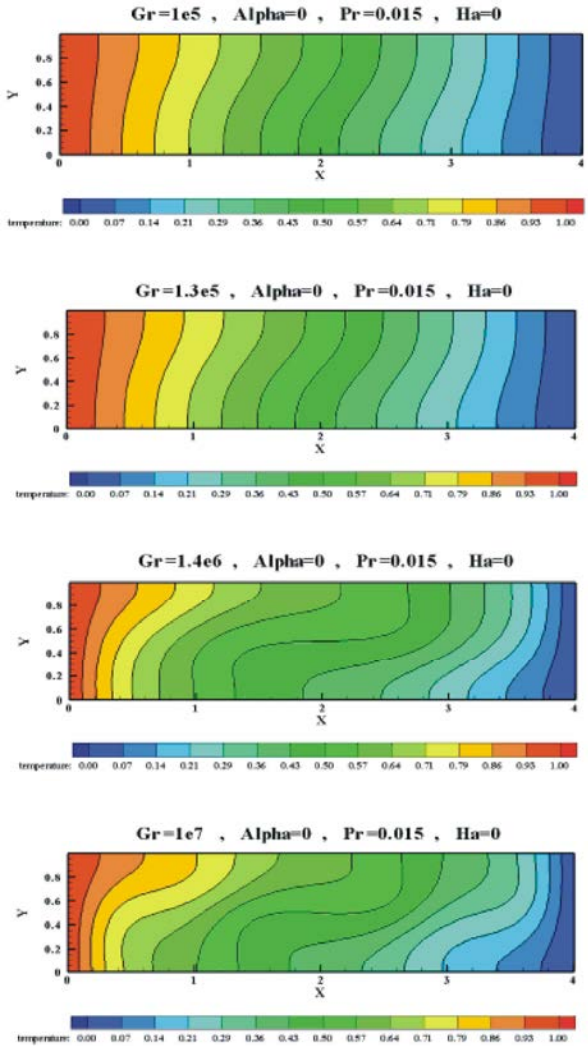

Fig. 3b: Effect of Grashof number on temperature field inside the cavity

recirculation region becomes smaller while two other vortex are beginning to develop at the right and left of the cavity. The size of these vortexes increases with increasing Gr number.

Fig. 3(b) illustrates the temperature field in the flow region. The high temperature region remains near the left side of the computational domain and the isothermal lines are nearly linear and parallel to the vertical walls for $Gr = 10^5$. These lines become more curved because of growing Gr. The isothermal lines concentrate near the hot and cold walls for larger values of Gr. As seen with increasing Grashof number the thickness of thermal boundary layer on the hot and cold walls decreases. Therefore, local heat transfer coefficient on the walls increase with increasing Grashof number.

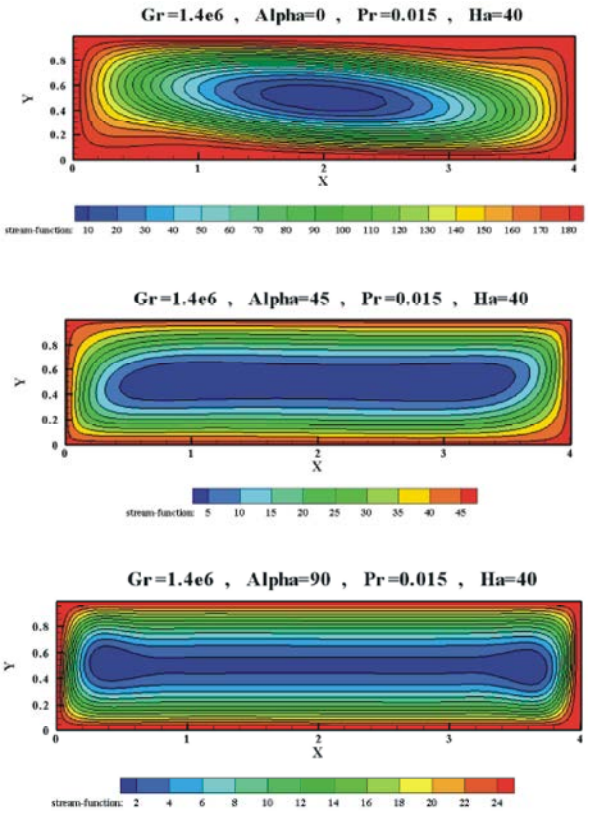

Fig. 4a: Effect of orientation of magnetic field on streamlines inside the cavity

The effect of orientation of magnetic field on the flow field is depicted in Fig. 4(a) where $Gr = 1.4\times10^6$, Pr = 0.015 and $Ha = 40$. The streamlines contain a rotating cell at $\alpha = 0$. The size of this vortex increases with increasing orientation of magnetic field so that it covers almost the whole cavity. Fig. 4(b) illustrates the temperature field in the flow region. The thermal field becomes more compressed at the hot and cold walls of the cavity with decreasing α. Furthermore, the high temperature region remains near the hot wall of the computational domain increases and the isothermal lines are become more linear and parallel to the vertical walls with increasing α. It is obvious that with increasing α the Nusselt number on the hot wall decreases because the thermal boundary layer on the wall increases.

Fig. 5(a,b) show the effect of Hartmann number Ha (from 0 to 80) on flow field at $Gr = 10^7$, Pr = 0.015, $\alpha = 0$. In the absence of magnetic field, the streamlines consist of two recirculation cells including one at the left side of cavity and a secondary eddy at the right side of cavity. As seen, these vortexes loss their strength and finally are disappeared with rising Ha while larger vortex produced

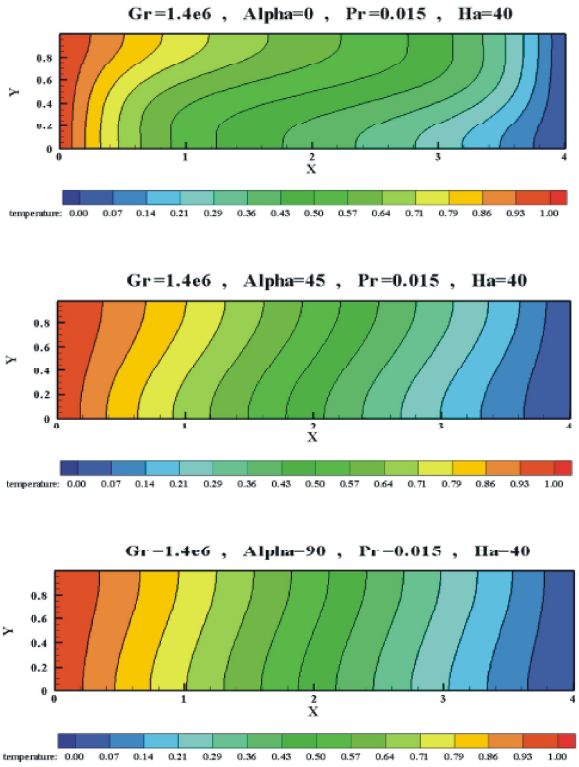

Fig. 4b: Effect of orientation of magnetic field on temperature field inside the cavity

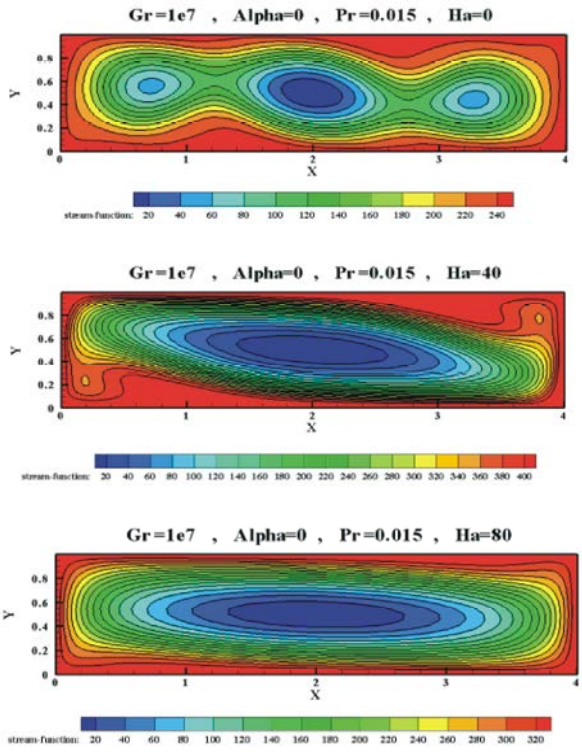

Fig. 5a: Effect of Hartmann number on streamlines inside the cavity

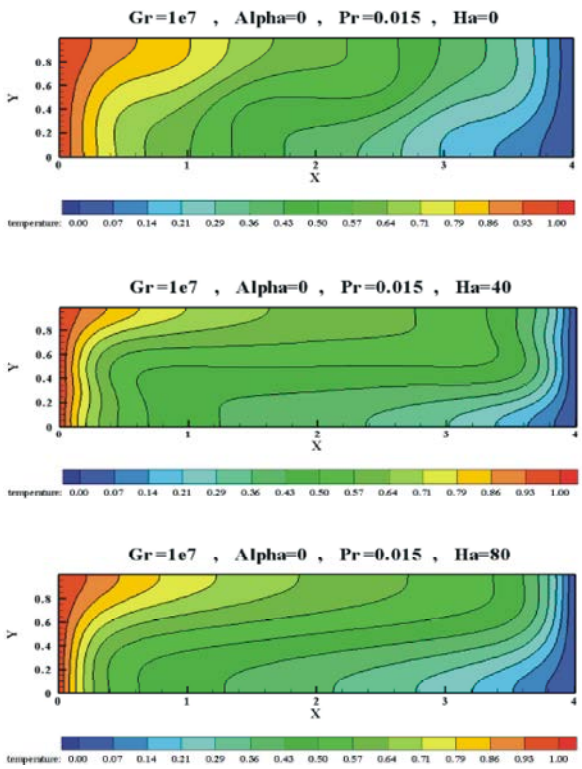

Fig. 5b: Effect of Hartmann number on temperature field inside the cavity

at the center of cavity. The corresponding temperature field shows that the concentrated region near the walls becomes more compressed and the isothermal lines are more bend from the right top corner due to the elevating Hartmann number. It means that the magnetic field significantly affects the flow and thermal fields in the cavity.

Fig. 6(a,b) show the effect of Prandtl number Pr on flow field at $Gr = 1.4\times10^6$, $Ha = 40$, $\alpha = 0$. As seen at both Prantdl numbers, the streamlines consist of a recirculation cell at the center of cavity but with rising Pr, the vortex become stronger and finally is covered the most of computational domain. The corresponding temperature field shows that the concentrated region near the walls becomes more compressed and the isothermal lines at the whole of domain except near vertical walls are become more linear and parallel to horizontal walls due to the elevating Prandtl number. It is clear that with increasing Prandtl number the thermal boundary layer on the walls decreases so the heat transfer coefficient on the walls increase.

In order to evaluate how the presence of Prandtl number, magnetic field and its orientation affects the heat transfer rate along the heated surface, the average Nusselt

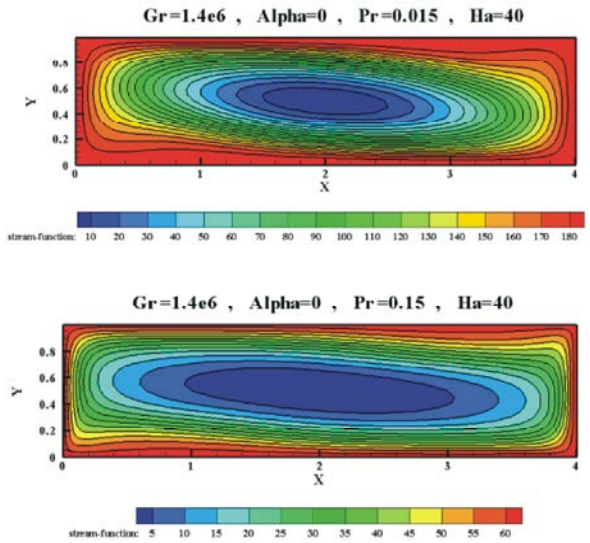

Fig. 6a: Effect of Prandtl number on streamlines inside the cavity

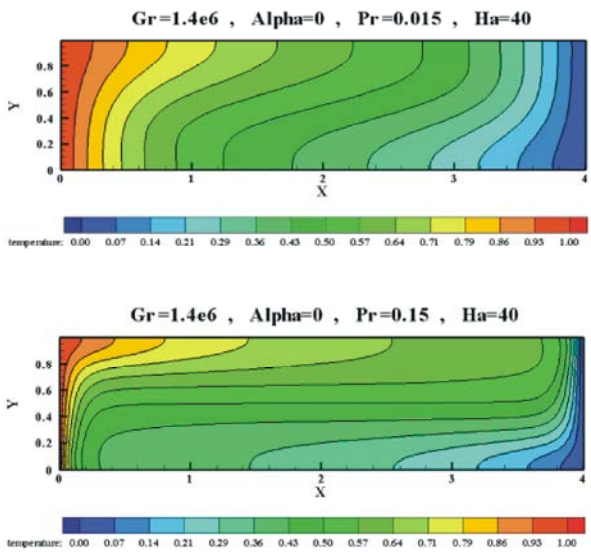

Fig. 6b: Effect of Prandtl number on temperature field inside the cavity

Table 3: Effect of α, Pr, *Gr*, *Ha* on Nusselt number

	Gr ⇒	10^5	1.3×10^5	1.4×10^6	10^7
$H\alpha = 40$	$\alpha = 0$	0.256	0.2616	0.5464	1.224
Pr = 0.015	$\alpha = 45$	0.2508	0.25103	0.2943	1.0487
	$\alpha = 90$	0.25067	0.2507	0.2650	0.6913
$\alpha = 0$	$H\alpha = 0$	0.2713	0.2792	0.5992	1.4027
Pr = 0.015	$H\alpha = 40$	0.256	0.2616	0.5464	1.224
	$H\alpha = 80$	0.2515	0.2523	0.3646	1.11062
$\alpha = 0$	Pr = 0.015	0.256	0.2616	0.5464	1.224
$H\alpha = 40$	Pr = 0.15	0.549	0.6533	2.6345	6.21144

number is plotted as a function of Grashof number as shown in Table 3. It is observed that Nu rises with increasing Grashof and Prandtl numbers and decreasing Hartmann and orientation of magnetic field. The maximum heat transfer rate is obtained for the lowest Ha and the highest Gr, because the magnetic field tends to retard the motion. It is worth mentioning that the influence of mentioned parameters on Nusselt number is not very sensitive at lower Grashof numbers.

CONCLUSIONS

In the present numerical investigation, we studied the effect of magnetic field on natural convection flow in a rectangular enclosure filled with an electrically conducting fluid. The enclosure is differentially heated at two opposite vertical walls while the horizontal walls are at adiabatic condition. The governing equations along the appropriate boundary conditions for the present problem are first transformed into a non-dimensional form and the resulting non linear system of partial differential equations are then solved numerically using finite volume method. the influence of Grashof number, Prantdl number of fluid, Hartmann number and orientation of magnetic field on the flow and heat transfer characteristic such as average Nusselt number, streamlines and isotherms is performed. It is observed that Nu rises with increasing Grashof and Prandtl numbers and decreasing Hartmann and orientation of magnetic field.

Nomenclature

C_p	Heat capacity of fluid at constant pressure $(J/kg.K)$
H	Height of cavity (m)
k	Thermal conductivity $(W/m.K)$
L	Length of cavity (m)
p	Pressure (pa)
$\hat{p}$	Non-dimensional pressure
Pr	Prandtl number
T	Temperature (K)
Nu	Nusselt number
Gr	Grashof number
Ha	Hartmann number
B	Magnetic field
g	Acceleration due to gravity
u,v	Velocity components in x and y directions (m/s)
$\hat{u},\hat{y}$	Non-dimensional velocity components in x and y directions
N_x, N_y	Number of grid in x and y directions

x, y Cartesian coordinates(m)
$\hat{x}, \hat{y}$ Non-dimensional Cartesian coordinates

Greek Symbols

α orientation angle of magnetic field
θ non-dimensional temperature
μ dynamic viscosity (kg/ms^2)
ρ density (kg/m^3)
β thermal expansion coefficient
σ electrical conductivity of fluid

Subscripts

h hot
c cold
$^\circ$ previous iteration
x in x direction
y in y direction
z in z direction

REFERENCES

1. Rudraiah, N., R.M. Barron, M. Venkatachalappa and C.K. Subbaraya, 1995. Effect of a magnetic field on free convection in a rectangular cavity, Int. J. Eng. Sci., 33: 1075-1084.
2. Pirmohammadi, M. and G.A. Ghassemi Sheikhzadeh, 2009. Effect of a magnetic field on buoyancy driven convection in differentially heated square cavity, IEEE Trans. Magn, 45(1): 407-411.
3. Sparrow, E.M. and R.D. Cess, 1961. The effect of a magnetic field on fre convection heat transfer, Int. J. Heat and Mass Transfer, 3: 267-274.
4. Lykoudis, P.S., 1962. Natural convection of an electrically conducting fluid in the presence of a magnetic field, Int. J. Heat and Mass Transfer, 5: 23-34.
5. Papailiou, D.D. and P.S. Lykoudis, 1968, Magnetofluid-mechanic laminar natural convection-and experiment, Int. J. Heat and Mass Transfer, 11: 1385-1391.
6. Papailiou, D.D. and P.S. Lykoudis, 1968. Magnetofluid-mechanic free convection turbulent flow, Int. J. Heat and Mass Transfer, 17: 1181-1189.
7. Seki, M., H. Kawamura and K. Sanokawa, 1979. Natural convection of mercury in a magnetic field parallel to the gravity, ASME J. Heat Transfer, 101: 227-232.
8. Fumizawa, M., 1980. Natural convection experiment with liquid NaK under transverse magnetic field, J. Nuclear Science and Technol., 17: 98-105.
9. Takhar, H.S., 1982. Dissipation effects on MHD free convection flow past a semi-infinite vertical plate, Applied Scientific Research, 36: 163-171.
10. Kim, K.M., 1982. Suppression of thermal convection by transverse magnetic field, J. the Electrochemical Society, 129: 427-429.
11. Langlois, W.E. and K. Lee, 1983. Czochralski crystal growth in an axial magnetic field: effects of joule heating, J. Crystal Growth, 62: 481-486.
12. Kerr, O.S. and A.A. Wheeler, 1989. The effect of a weak vertical magnetic field on the buoyancy-driven boundary-layer flow past a vertical heated wall, J. Fluid Mechanics, 199: 217-236.
13. Okada, K. and H. Ozoe, 1992. Experimental heat transfer rates of natural of molten gallium suppressed under an external magnetic field in either the X, Y or Z direction, ASME J. Heat Transfer, 114: 107-114.
14. Barth, T.J. and D. Jesperson, 1989. The Design and Application of Upwind Schemes on Unstructured Meshes, AIAA Paper No.89-0366.
15. Leonard, B.P., 1995. Order of Accuracy of Quick and Related Convection-Diffusion Schemes, Appl. Math. Model., 19: 640.
16. Vandoormall, J.P. and G.D. Raithby, 1984. Enhancements of the Simple Method for Predicting Incompressible Fluid Flow, Numerical Heat Transfer, 7: 147-163.
17. Davis, G.D.V., 1983. Natural convection of air in a square cavity: a benchmark solution, Int. J. Numer. Meth. Fluids, 3: 249-264.
18. Markatos, N.C. and K.A. Pericleous, 1984. Laminar and turbulent natural convection in an enclosed cavity, Int. J. Heat Mass Transfer, 27: 755-772.
19. Hadjisophocleous, G.V., A.C.M. Sousa and J.E.S. Venart, 1998. Predicting the transient natural convection in enclosures of arbitrary geometry using a no orthogonal numerical model, Numer. Heat Transfer A, 13: 373-392.